# Energy Harvester and Cell Proliferation from Biocompatible PMLG Nanofibers Prepared Using Near-Field Electrospinning and Electrospray Technology

Cheng-Tang Pan[1], Chung-Kun Yen[1], Shao-Yu Wang[1], Shih-Kang Fan[2], Fong-Yi Ciou[1],
Liwei Lin[3], J. C. Huang[4], and Shiao-Wei Kuo[4, *]

[1] Department of Mechanical and Electro-Mechanical Engineering, National Sun Yat-Sen University, Kaohsiung 80424, Taiwan
[2] Department of Mechanical Engineering, National Taiwan University, Taipei, 10617, Taiwan
[3] Department of Mechanical Engineering, University of California, Berkeley, California 94720, USA
[4] Department of Materials and Optoelectronic Science, Center for Nanoscience and Nanotechnology,
National Sun Yat-Sen University, Kaohsiung 80424, Taiwan

This paper describes the application of piezoelectric fibers and films formed using near-field electrospinning (NFES) and electrospray (ESP) technology. Poly($\gamma$-methyl L-glutamate) (PMLG), a biocompatible material, was mixed with poly(ethylene oxide) (PEO) and surfactant to obtain a solution of appropriate viscosity and conductance. Because the orientation of the dipoles in PMLG was enhanced upon applying an electric field, we could use the NFES and ESP processes to align dipoles and enhance the piezoelectric properties of the resulting fibrous materials. The maximum peak voltage of a fiber-based harvester prepared using this approach was 0.056 V. Because the fibers and films were non-toxic biological materials displaying excellent piezoelectric characteristics, we deposited them on glass substrates coated with indium tin oxide to observe their effects on the proliferation of cells. The negative charge of PMLG decreased the proliferation of mouse fibroblast cells (NIH3T3); indeed, decreasing the interspacing between the fibers slightly decreased the proliferation of these cells. Moreover, the migration of the cells was inhibited significantly, or even halted, when the coverage of the ESP films increased, implying a growth inhibition effect.

**Keywords:** Nanofiber, Polypeptide, Electrospinning, Electrospray, Piezoelectric Materials.

## 1. INTRODUCTION

Progress in micro electro-mechanical technology has been growing rapidly with many studies focused on low-energy devices and biomedical engineering (e.g., biosensors; biological cultivation). Nevertheless, such applications have remained rare, in part due to high costs.

Polymer piezoelectric materials are typically inexpensive and readily fabricated. Crystalline piezoelectric materials can convert mechanical strain into electrical charge.[1] Near-field electrospinning (NFES)[2,3] can be used to fabricate controllable fibers with diameters ranging from micrometers to nanometers.[4] The NFES process can be used synthetically to prepare polymer alloys and composites as well as biopolymers.[5] These electrospun fibers can display many attractive characteristics, including small diameters, high porosities, and high surface-to-volume ratios.[6] In this study, NFES and electrospray (ESP) processes were used to fabricate fibers and films based on poly($\gamma$-methyl L-glutamate) (PMLG). After electrospinning and spreading under a high electric field, the $\alpha$-helix of a polyglutamate can rearrange to enhance its piezoelectric properties.[7,8] The peptide group in this polymer and the side-chain esters of PMLG can derive the equilibrium number of hydrogen bonding interactions.[9,10]

The physicochemical properties of scaffold materials are critically important in tissue engineering for regulating cell behaviour and the interactions among cell materials.[11–13] Extracellular matrices having fibrous nanoscale morphologies and biomimicking characteristics have been used to cause beneficial effect in tissue regeneration engineering.[14] Biodegradability is a particularly promising scaffolding materials, poly(ethylene

*Author to whom correspondence should be addressed.

oxide) (PEO), with its unique material for tissue engineering.[15–17]

Electrospinning is the simple but multifunctional method for manufacturing nanofibers. Fibers from various polymer solutions can be electrically spun (via Taylor cones) onto substrates at nano-scale diameters.[18] Traditional electrospinning can, however, be unstable or chaotic, leading to disordered or randomly aligned fibers.[19] Continuous NFES was established as a superior technique because its precise positioning control allows the deposition of nanofibers with sophisticated patterns.[20] Scaffolding systems presenting nanofibers prepared through electrospinning can be used to achieve excellent cell alignment.[21] The cellular interactions within the prescribed microscale patterns of nanofibers can be characterized in terms of cellular alignment and related tissue architecture.[22] Binary micro- and nanoscale technology has recently opened up new territories for studying associated biological effects (e.g., assessing dose effects quantitatively; relating the size-dependence responses of new nanomaterial-based assays).[23, 24]

In this present study, we used NFES and ESP processes to prepare direct-write fibers and spread films, respectively, to observe the cell proliferation. The NFES has been demonstrated to be able to achieve direct-write and highly-aligned fibers with prescribed positioning density. After determining the most suitable recipe for the PMLG solutions blended with PEO and surfactant, we formed fibers and films from them to characterize their cellular biocompatibility and cell proliferation phenomena (i.e., cell

spreading and extension guided in a preferential direction). Cell growth in fiber direction could be observed, and the electrosprayed films were capable of affecting cell extension. These maskless, and direct-write patterns could be fast fabricated and be a promising tool to study the cell-based research.

## 2. EXPERIMENTAL SECTION

### 2.1. Materials
PMLG was synthesized with a molecular weight ($M_w$) of 11,020;[25, 26] PEO with a value of $M_w$ of 10,000 was purchased from Aldrich (USA), the cell, NIH3T3 (ATCC CRL-1658™) is purchased from ATCC, and the surfactant (Zonyl Fluoro-surfactant) is purchased from DuPont Company. The as-fabricated fibers and films were manipulated under ambient conditions. During the NFES and ESP processes, the electric field was controlled to form the PMLG droplet, induce the repulsive force, and form the Taylor cone, thereby fabricating the ordered fibers and films.

### 2.2. Solution Concentration
PMLG-based solutions for NFES and ESP process were formulated as follows. PMLG was dispersed in dimethyl-formamide to obtain a solution having a concentration of 21.05 wt%. This PMLG solution was mixed with PEO and surfactant to form a ternary PMLG/PEO/surfactant = 1/1/0.05 solution for NFES and 1/1/0.5 for ESP process having conductivity greater than those of pure PMLG and binary PMLG/PEO solutions.
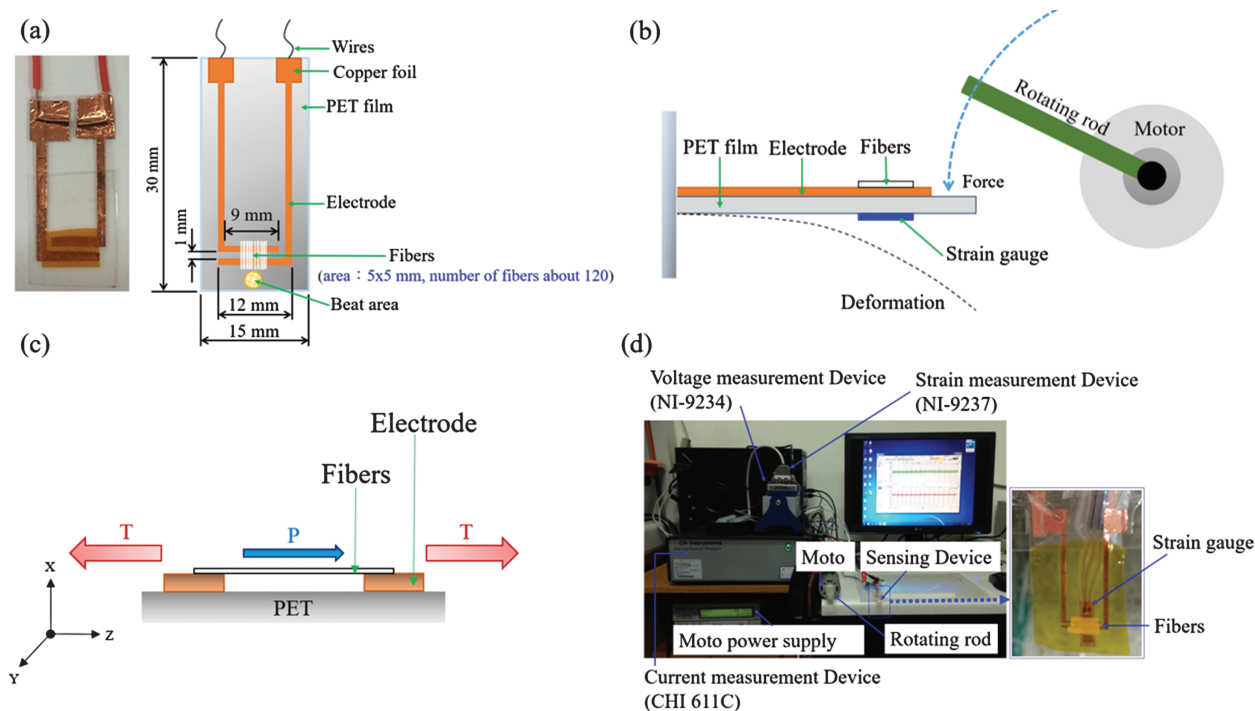
**Scheme 1.** Schematic representations of (a) a PET sensing device, (b) the vibration test, (c) the piezoelectric {3–3} mode, and (d) the vibration measurement system.

## 2.3. NFES and ESP Processes

NFES and ESP processes were employed to fabricate the direct-write fibers and uniformly spread films, respectively. The experimental setup included a needle clamping apparatus, a high electric field power supply ($12 \times 10^6$ V/m), an infusion pump (1 mL/h advancing speed), a collection plate, an NC controller (60 mm/s moving rate), and gaps between the needle and collection plate of 0.5 mm for NFES and 10 mm for ESP.

## 2.4. Mechanical Strain Rate to Induce Electric Potential

The PMLG-based harvester was used to transform mechanical vibration energy into electrical energy. The PMLG fibers of the harvester existed in an area of 5 mm × 5 mm with a fiber count of approximately 120. The harvester was attached atop a flexible film of poly(ethylene terephthalate) (PET). Both ends of the harvester were bonded to parallel copper electrodes to examine the voltage output of this transducer. A schematic representation of the vibrational harvester is presented in Scheme 1(a). Mechanical stress from compressive and tensile stress can induce charges in the fibers. A schematic representation of the vibration measurement system is displayed in Scheme 1(b). The harvester was examined by applying a DC motor to observe the displacement of the harvester under periodic external strain. The bending effect resulted in mechanical strain that was distributed along the fibers and then transformed to an alternative voltage via the piezoelectric {3–3} mode [Scheme 1(c)]. Scheme 1(d) displays a schematic representation of the measurement system, where a rod was connected to a rotary motor operated at low frequency. The rod tapped the harvester at the free end to induce axial strain and a voltage along the fibers. With different frequencies of the rod tapping on the harvester, the voltage and strain could be induced and analyzed.

## 2.5. Cell Culture and Applications

Cells were grown in 90% Dulbecco's modified Eagle's medium (DMEM) and 10% Tet system approved fetal bovine serum (FBS) at 37 °C in a presence of 5% $CO_2$. The spun fibers and spread films were deposited on a substrate of ITO-coated glass. To observe cell proliferation, the cell suspension was added to the fibers and films in a sterile dish and cultured.

## 3. RESULTS AND DISCUSSION

The PMLG solution for NFES was filled into a syringe featuring a needle tip of 0.15-mm internal diameter (needle gauge: 30G). An electric field of $12 \times 10^6$ V/m was applied at the gap between the collector and the syringe tip; the gaps were set as 0.5 mm for NFES and 10 mm for ESP. To control the condition of the fibers and films, the substrate was held on an NC controller. When the electrical
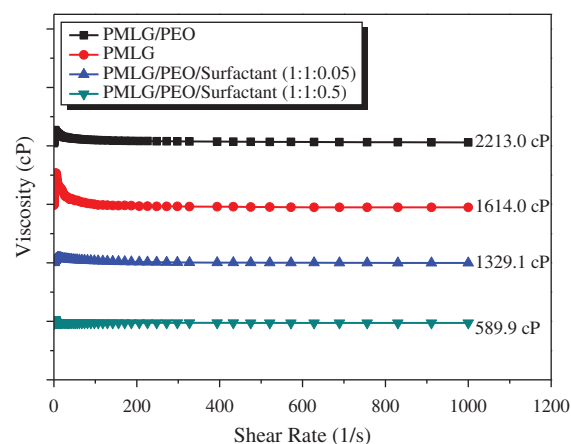


**Figure 1.** Relationship between shear rate and viscosity.

field overcame the droplet surface tension, fibers could be spun from the Taylor cone. Using this approach, fibers with well-aligned piezoelectricity were directly patterned on the ITO-coated glass. At an appropriate viscosity and surface tension, the PLMG solution could be used to fabricate controllable fibers and films. If the concentration of the PMLG solution was too high, its heavy viscous resistance resulted in difficulty spreading.

## 3.1. Solutions of Viscosity and Conductivity

In Figure 1, the viscosity of the pure PMLG solution was 1614.0 cP. After adding the high-molecular-weight PEO homopolymer, the viscosity of the PMLG solution increased to 2213.0 cP. Because this greater viscosity might have caused needle blockage, we added a surfactant to change the surface tension of the solution. When the PMLG solution was mixed with appropriate proportions of PEO and surfactant (PMLG/PEO/Surfactant = 1/1/0.05), the PMLG fibers could be fabricated successfully (solution viscosity: 1329.1 cP). Notably, adding too much surfactant (PMLG/PEO/Surfactant = 1/1/0.5) resulted in the viscosity being too low (589.9 cP) to fabricate PMLG fibers. The conductances of the pure PMLG solution, the
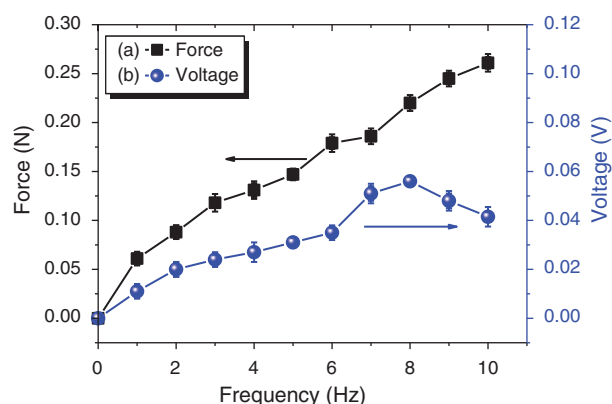


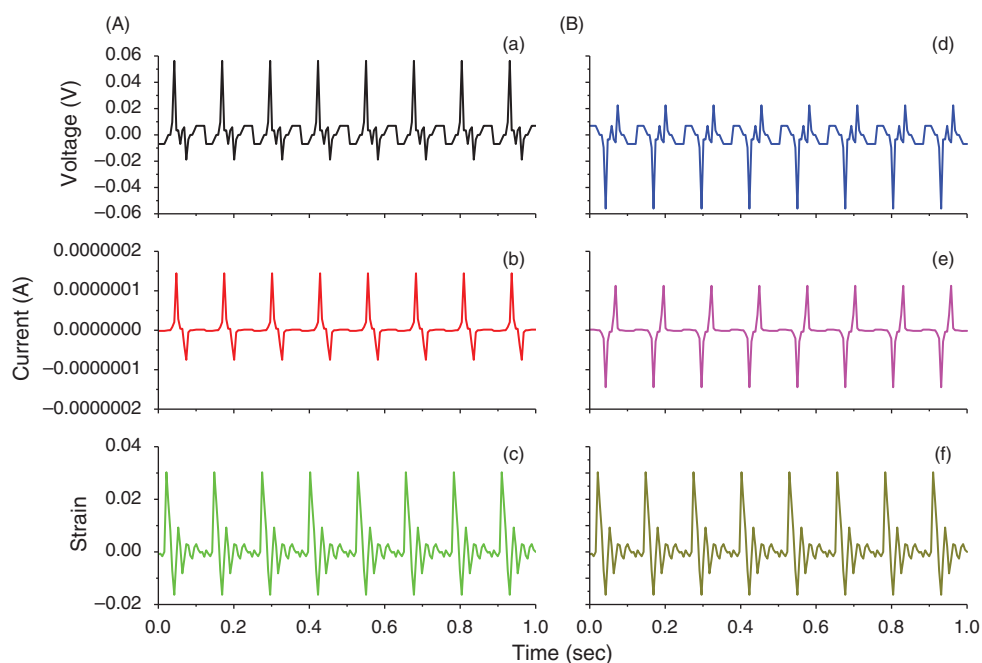**Figure 2.** Relationship between frequency with (a) force and (b) voltage.

**Figure 3.** PMLG electrical measurements: (A) positive and (B) reverse connections: (a) voltage, (b) current, and (c) strain.

PMLG/PEO solution, and the PMLG/PEO/surfactant solution were 30.83, 31.21, and 98.96 $\mu$S/cm, respectively. Thus, adding both PEO and surfactant increased the conductance to three times greater than that of the pure PMLG solution.

### 3.2. Harvester Measurement Under Low-Frequency Vibration

In this study we prepared a harvester that could be operated at low frequency. We measured the electric current,

voltage, and strain from the harvester at vibrational frequencies of 1–10 Hz. As the frequency increased from 1 to 10 Hz, the force increased from 0.06 to 0.26 N (Fig. 2(a)), with the output voltage of the harvester within the range from 0.011 to 0.0415 V (Fig. 2(b)). The voltage did not, however, increase without limit with respect to the frequency because high frequencies made it difficult for this flexible PET-based harvester to recover completely, thereby decreasing the output voltage. Consequently, we chose a frequency of 8 Hz for subsequent
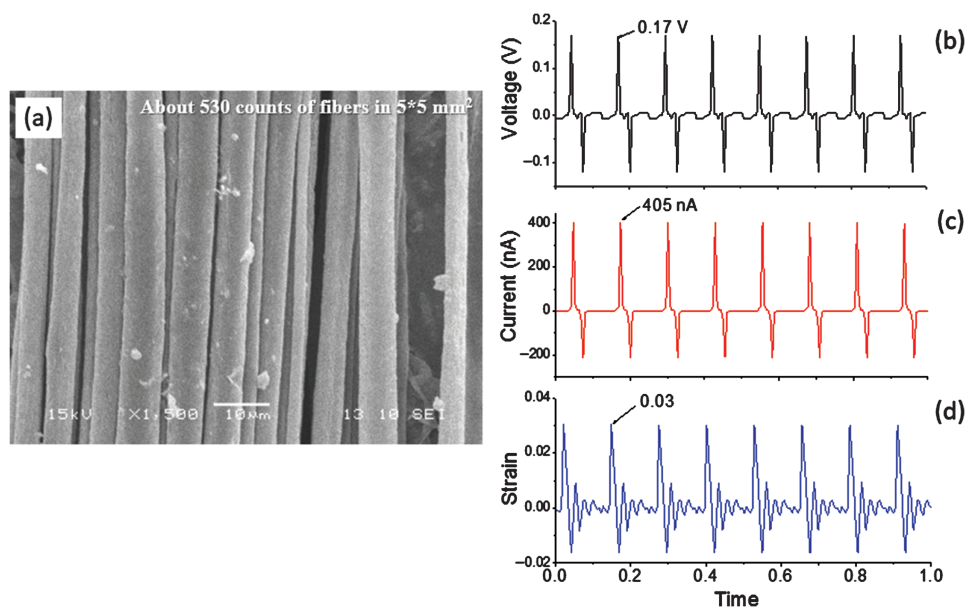
**Figure 4.** SEM image and electrical measurements of PMLG fibers: (a) the area of 5 mm × 5 mm with a fiber count of approximately 530 SEM image, (b) voltage, (c) current, and (d) strain.
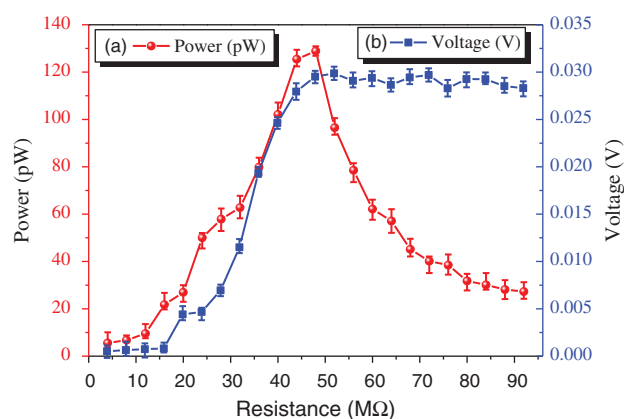
**Figure 5.** PMLG impedance matching test.

electrical measurements. Figure 3 displays the responses of the induced electric potentials as a periodic force was applied at 8 Hz to the harvester. The peak electric current was $1.39 \times 10^{-7}$ A, with a maximum voltage of 0.056 V at a strain of 0.03. For this result, only few fibers are fabricated on 5 mm × 5 mm in area, it is about 120 counts of fibers. Though the maximum peak voltage of this harvester was 0.056 V, it can be enhanced by adding more fibers. A higher voltage of 0.17 V can be obtained when fiber counts were increased, as shown in Figure 4.

### 3.3. Power Generation of Harvesters

PMLG fibers were deposited on a PET substrate and packaged as a harvester. Both ends were bonded to copper

parallel electrodes. Colloidal silver gels were applied at both fibers ends to hold the ends together tightly. This structure allowed the induction of a voltage and electric current pulse. Furthermore, the harvester was configured with an impedance matching test with an external load resistor (RL) of 46 MΩ. Upon periodic stretching and release, this harvester produced a peak voltage and power of 0.032 V and 168.54 pW, respectively, at a strain of 0.03 and a frequency of 8 Hz, as displayed in Figure 5.

### 3.4. Optimal Parameters of Fibers and Films Prepared Using NFES and ESP Processes

Unlike the far-field electrospinning (FFES) process, the higher electrical fields and the stronger mechanical stretching conditions of the NFES process can induce alignment of the dipoles of the fibers. Therefore, the NFES process allows fibers to be fabricated with relative smaller diameters, smoother surface structures, and excellent piezoelectricity. We fixed the infusion pump rate at 1 mL/h for the NFES and ESP process. If the speed of the movement of the NC table was too slow, the fibers might form beads or possess larger diameter; in contrast, a higher speed might lead to finer, more uniform fibers. Hence, we set the collection rate at 60 mm/s.

The magnitude of the electric field, the speed of NC controller, the concentration of the solution, and the diameter of the needle were the parameters that we varied to control the diameter of the electrospun fibers. We changed one parameter at a time during the NFES process to determine
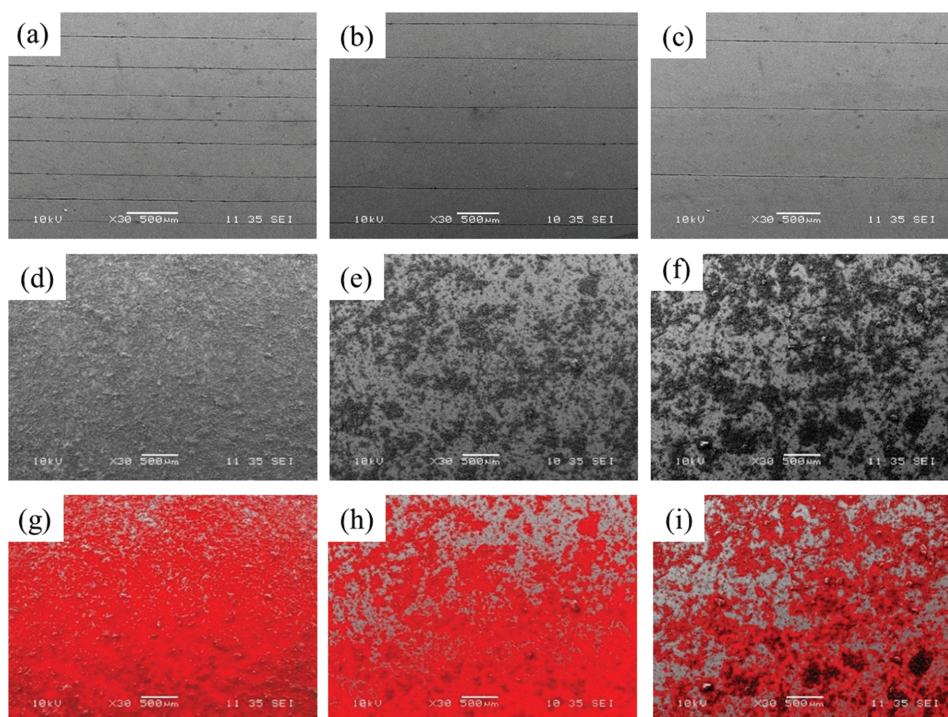


**Figure 6.** SEM images of (a–c) fibers with spacings of (a) 250, (b) 500, and (c) 750 $\mu$m and (d–i) ESP-deposited films (film coverages) of (d, g) 250 $\mu$m (89.55%), (e, h) 500 $\mu$m (62.13%), and (f, i) 750 $\mu$m (41.05%).
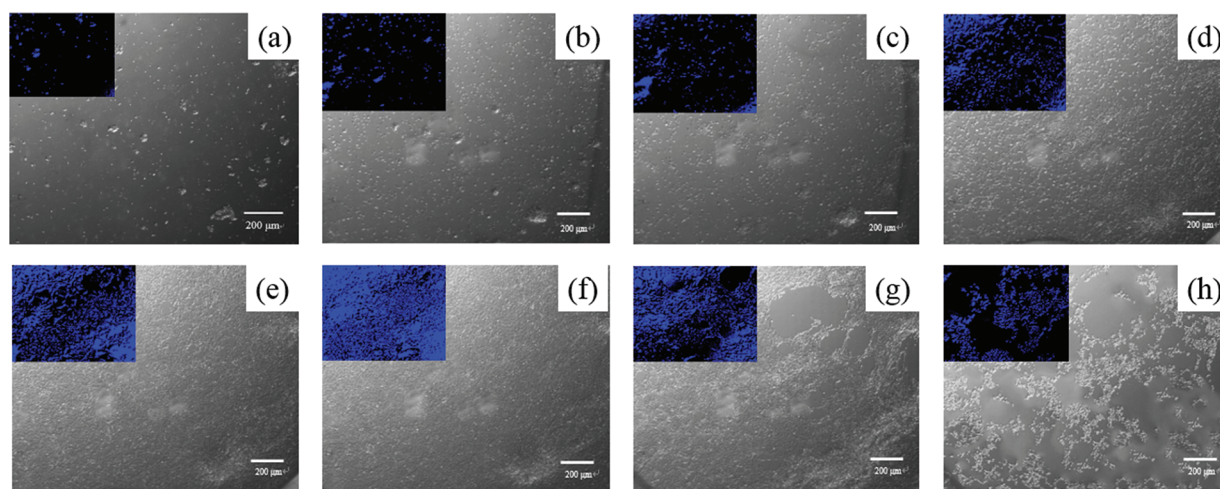
**Figure 7.** SEM images (cell coverages) of (a) NIH3T3 cells (2.87%) and (b–h) NIH3T3 cells cultured on a blank substrate for (b) 0.5 days (4.62%), (c) 1 day (7.71%), (d) 2 days (37.11%), (e) 3 days (56.85%), (f) 4 days (91.21%), (g) 5 days (43.36%), and (h) 6 days (16.90%), where the blue color images in the inset represent the cell coverage.

its effect on the fiber diameter. When we set the gap between the collector and needle at 0.5 mm and the electric field at $12 \times 10^6$ V/m, we found that the NFES and ESP processes were affected by the size of the needle. In these experiments, the optimal needle was one having an internal diameter of 0.15 mm (needle gauge: 30G) for the electrospinning process.

When the gap between the needle and collection plate was less than 0.5 mm, too high an electric field tended to cause the collection plate to short-circuit. Thus, an

appropriate electric field was necessary to fabricate more uniform, smaller-diameter fibers when the gap between the needle and the collection plate was set at 0.5 mm. Too low an electric field made the films uneven when the gap between the needle and the collection plate was greater than 10 mm. An appropriate electric field transformed the droplets into a Taylor cone and resulted in uniform films. For the electrospinning process, we obtained more uniform and continuous fibers when the electric field was near $12 \times 10^6$ V/m. Figures 6(a)–(c) present SEM images
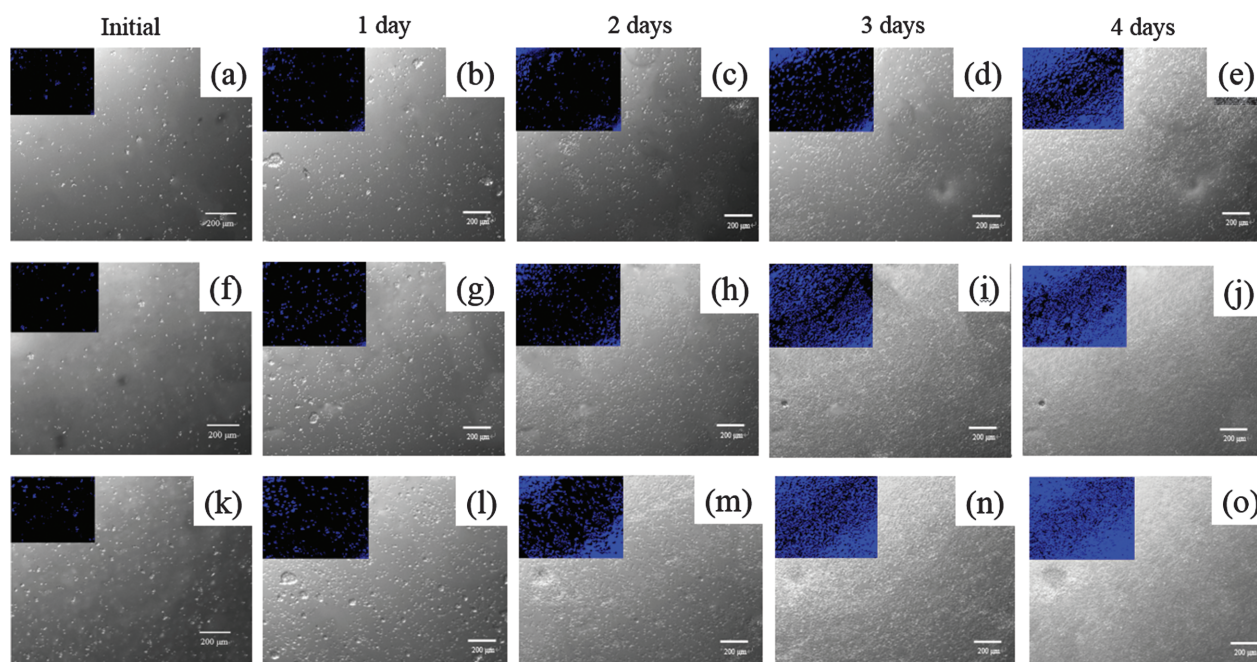


**Figure 8.** SEM images and cell coverage of NIH3T3 on fibers spacing were 250 $\mu$m to cell culture in: (a) initial (2.43%), (b) 1 day (4.51%), (c) 2 days (8.55%), (d) 3 days (21.36%), (e) 4 days (66.42%), 500 $\mu$m to cell culture in: (a) initial (2.04%), (b) 1 day (5.13%), (c) 2 days (11.64%), (d) 3 days (47.86%), (e) 4 days (72.73%), 750 $\mu$m to cell culture in: (a) initial (2.59%), (b) 1 day (7.14%), (c) 2 days (36.81%), (d) 3 days (62.06%), (e) 4 days (88.38%), where the blue color images in the inset represent the cell coverage.
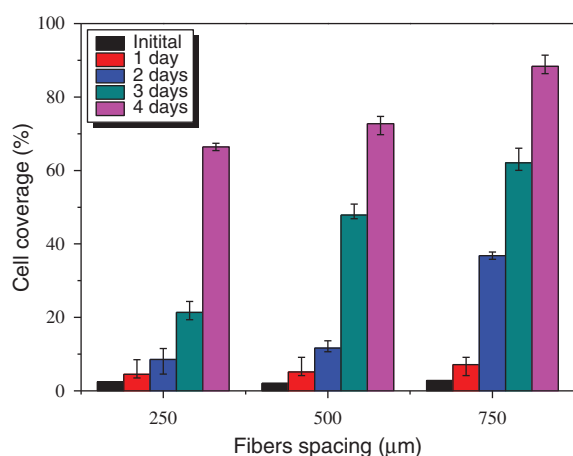
**Figure 9.** Cell coverage after 4 days plotted with respect to fiber spacing.



**Figure 11.** Cell coverage after 4 days plotted with respect to the film coverage.

of as-spun fibers with various interspacings (250, 500, and 750 $\mu$m). The ITO-coated glass was adopted as a substrate (area: 40 mm × 40 mm). We used an electric field of $12 \times 10^6$ V/m to fabricate films with various coverages under conditions providing various interspacings (Figs. 6(d–f)). Figures 6(g)–(i) reveal that the coverages were 41.05–89.55%, as determined using Image J software.

### 3.5. Cell Proliferation

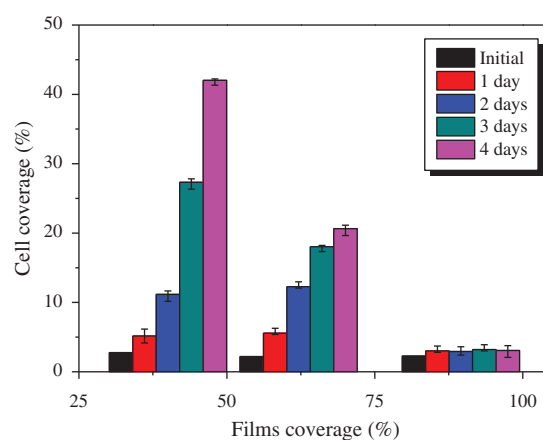For our study of cell proliferation, we used NIH3T3 cells because they were easy to grow and attach; we used Image

J (v. 1.38×) for image analysis. In time-cell activity, the cell activity from initial to late stage increased initially and then decreased. We cultured the NIH3T3 cells on a blank substrate for 1–6 days. The initial NIH3T3 coverage was 2.87% (Fig. 7(a)); the cell coverage increased (to 4.62% then 37.11%) after 1–2 days (Figs. 7(b–d)); it increased further (42.19%–91.21%) after 3–4 days, reaching saturation (Figs. 7(e and f)). The NIH3T3 cells contracted and died (cell coverage: from 43.36 to 16.90%) after 5–6 days (Figs. 7(g and h)). Because the cultured NIH3T3 cells lacked nutrient and died after 5–6 days, we performed follow-up tests within 1–4 days in subsequent experiments.
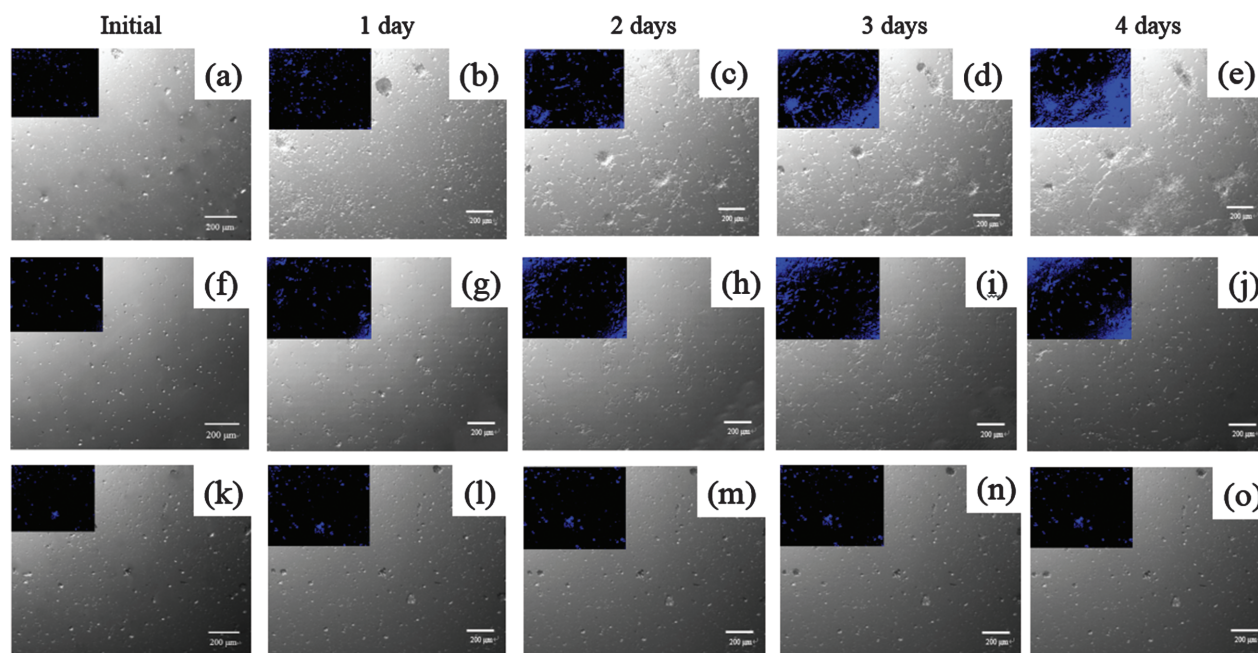
**Figure 10.** SEM images and film coverage of NIH3T3 on 41.05% to cell culture in: (a) initial (2.77%), (b) 1 day (5.16%), (c) 2 days (11.16%), (d) 3 days (27.33%), (e) 4 days (42.03%), 62.13% to cell culture in: (a) initial (2.19%), (b) 1 day (5.58%), (c) 2 days (12.27%), (d) 3 days (18.03%), (e) 4 days (20.64%), 89.55% to cell culture in: (a) initial (2.27%), (b) 1 day (3.01%), (c) 2 days (2.92%), (d) 3 days (3.21%), (e) 4 days (3.07%), where the blue color images in the inset represent the cell coverage.
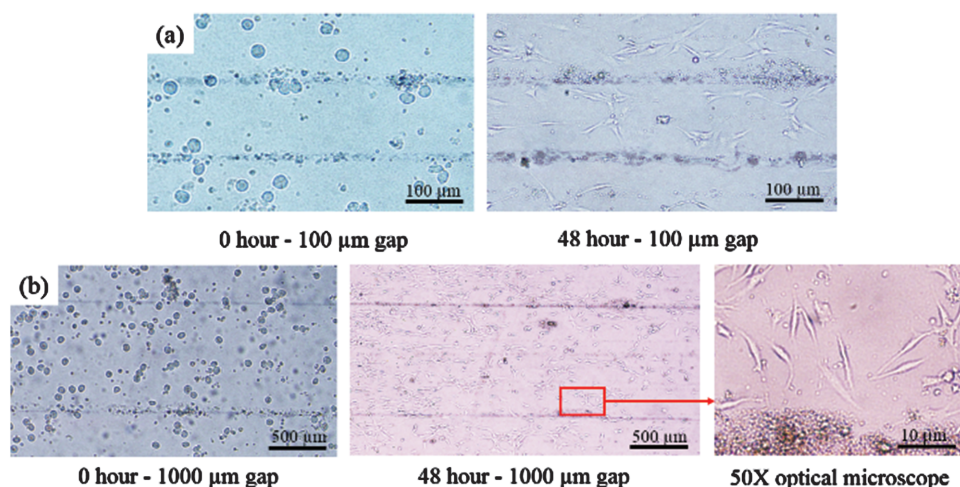
**Figure 12.**   The evolvement of cells culture near PMLG fibers, (a) the pitch is set as 100 $\mu$m, (b) the pitch is set as 1000 $\mu$m.

Figure 8 displays the results of NIH3T3 cell cultures when using PMLG fibers having various interspacings (250, 500, and 750 $\mu$m). When the interspacing was 250 $\mu$m, the initial coverage of NIH3T3 cells was 2.43% (Fig. 8(a)); the cell proliferation rate was slow, reaching a cell coverage of 66.42% after 4 days (Fig. 8(e)). When the interspacing was increased to 500 $\mu$m, the initial coverage of NIH3T3 cells was 2.04% (Fig. 8(f)); it reached 72.73% after 4 days (Fig. 8(j)). When we increased the interspacing further, to 750 $\mu$m, the initial coverage of NIH3T3 cells (2.59%; Fig. 8(k)) reached 88.38% after 4 days. Figure 9 plots the relationship between the fiber interspacing and cell proliferation after 4 days. Decreasing the interspacing between the as-prepared fibers led to a slight decrease in the proliferation of NIH3T3 cells.

Figure 10 displays the effect of film coverage on the NIH3T3 cell cultures. When the film coverage was 41.05%, the initial coverage of NIH3T3 cells (2.77%; Fig. 10(a)) increased to 42.03% after 4 days (Fig. 8(e)). When the film coverage was 62.13%, the initial coverage of NIH3T3 cells was 2.19% (Fig. 8(f)), increasing to 20.64% after 4 days (Fig. 10(j)). When the film coverage was 89.55%, the initial cell coverage of 2.27% (Fig. 10(k)) transformed from 1 to 4 days to only 2–3% (Figs. 10(l~o)). Figure 11 plots the relationship between the films coverage and cell proliferation after 4 days. The migration of NIH3T3 cells was inhibited significantly, or even halted, upon increasing the coverage of the ESP film.

In this study we used NFES and ESP processes to fabricate direct-write fibers and spread films. These fibers and films greatly influenced cell proliferation. Both the film coverage and the fiber interspacing were primary factors affecting cell proliferation. Because PMLG was possessed hydrogen bonding wherein the hydrogen bond possessed a strong negative charge, it could affect cell viability and, thus, cell proliferation. From the Kato et al. study, they reported that amino, alkyl and hydroxyl terminal groups were introduced into PMLG particles to obtain aminated PMLG (cationic microcarriers), alkylated PMLG (neutral-based microcarriers) and hydroxyl terminated PMLG (neutral-based microcarriers), respectively. Many factors could affect cell growth such as hydrophobicity, length of functional groups, and anion exchange capacity (AEC).[27, 28] The PMLG fibers is spun and collected on the collector. After this process, the PMLG fibers carried negative charges. Then the PMLG fibers are used to culture and observe the cell growth. The preliminary results show the cell growth is inhibited by the negative-charged fibers. But, there are so many important factors such as surface properties and AEC involved in the cell growth mechanism. At this stage, they were not characterized in this study yet. But the authors could analyze some of those effects on cell growth in the near future. The current result could be helpful in further understanding of PMLG fibers microcarriers for the culture of cells.

In addition, various PMLG pitches were spun on ITO substrate, then cells were inoculated and cultured to observe their development around the fibers. Figure 12(a) shows when the pitch is set as 100 $\mu$m, the cell development was inhibited near the fibers clearly where the cell could not proliferate near the fibers. In addition, another pitch of 1000 $\mu$m was carried out. The same result can be observed in Figure 12(b). The cells were cultured on ITO substrate with the PMLG fibers. For a period of hours, the cells could not proliferate and spread on the fibers.

## 4. CONCLUSIONS

In this study we filled a PMLG solution for NFES into a syringe featuring a needle tip having an internal diameter of 0.15 mm (needle gauge: 30G). We applied an electric field of $12 \times 10^6$ V/m at a gap between the collector and the syringe tip; the optimal gaps were 0.5 mm for the NFES process and 10 mm for the ESP process. Under these conditions, the electrical field overcame the droplet surface tension, allowing fibers to be spun from the

Taylor cone. Accordingly, we could directly pattern fibers with well-aligned dipoles onto ITO-coated glass. When we applied a tapping force of 8 Hz to the harvester, the peak electric current was $1.39 \times 10^{-7}$ A, with a maximum voltage of 0.056 V at a strain of 0.03. The harvester was configured with the matching impedance of an external load resistor of 46 M$\Omega$; it could produce a power of 168.54 pW. We used the NFES and ESP processes to fabricate direct-write fibers and spread films. The as-spun fibers and films influenced cell proliferation significantly. The film coverage and the fiber interspacing on the substrate were two main factors affecting cell proliferation. Since PMLG was possessed hydrogen bonding, which possessed a strong negative charge, it could affect cell viability.

## References and Notes

1. I. Iliuk, J. M. Balthazar, A. M. Tusset, J. L. P. Felix, and B. R. Pontes, *Diff. Equat. Dynamic Sys.* 21, 93 (**2013**).
2. D. Sun, C. Chang, S. Li, and L. Lin, *Nano Lett.* 6, 839 (**2006**).
3. C. Chang, K. Limkrailassiri, and L. Lin, *Appl. Phys. Lett.* 93, 123111 (**2008**).
4. Z. H. Liua, C. T. Pan, L. W. Lin, and H. W. Lai, *Sensor Actuat. A-Phys.* 193, 13 (**2013**).
5. A. Greiner and J. H. Wendorff, *Angew. Chem. Int. Ed.* 46, 5670 (**2007**).
6. Z. M. Huang, Y. Z. Zhang, and K. S. Ramakrishna, *Compos. Sci. Technol.* 63, 2223 (**2003**).
7. C. T. Pan, C. K. Yen, Z. H. Liu, and H. W. Li, *Sensors Mater.* 26, 63 (**2014**).
8. C. T. Pan, C. K. Yen, L. W. Lin, Y. S. Lu, H. W. Li, C. C. Jacob, and S. W. Kuo, *RSC Adv.* 4, 21563 (**2014**).
9. P. C. Painter, W. L. Tang, J. F. Graf, B. Thomson, and M. M. Coleman, *Macromolecules* 24, 3929 (**1991**).
10. C. T. Pan, C. K. Yen, H. C. Wu, L. W. Lin, Y. S. Lu, J. C. C. Huang, and S. W. Kuo, *J. Mater. Chem. A* 3, 6835 (**2015**).
11. Y. K. Fuh, S. Z. Chen, and Z. Y. He, *Nanoscale Res. Lett.* 8, 97 (**2013**).
12. P. X. Ma, *Adv. Drug Delivery Rev.* 60, 184 (**2008**).
13. H. Shin, S. Jo, and A. G. Mikos, *Biomaterials* 24, 4353 (**2003**).
14. S. D. McCullen, S. Ramaswamy, L. I. Clarke, and R. E. Gorga, *WIRE: Nanomedicine and Nanobiotechnology* 1, 369 (**2009**).
15. D. H. Reneker and I. Chun, *Nanotechnology* 7, 216 (**1996**).
16. J. Han, J. F. Zhang, R. X. Yin, G. P. Ma, D. Z. Yang, and J. Nie, *Carbohydrate Polym.* 83, 270 (**2011**).
17. X. W. Fan, L. J. Lin, and P. B. Messersmith, *Biomacromolecules* 7, 2443 (**2006**).
18. W. E. Teo and S. Ramakrishna, *Nanotechnology* 17, 89 (**2006**).
19. J. D. Schiffman and C. L. Schauer, *Biomacromolecules* 8, 2665 (**2007**).
20. Y. K. Fuh, S. Z. Chen, and J. S. C. Jang, *J. Macromol. Sci. Part A: Pure Appl. Chem.* 49, 845 (**2012**).
21. S. A. Sell, M. J. McClure, K. Garg, P. S. Wolfe, and G. L. Bowlin, *Adv. Drug Delivery Rev.* 61, 1007 (**2009**).
22. Y. Orlova, N. Magome, L. Liu, Y. Chen, and K. Agladze, *Biomaterials* 32, 5615 (**2011**).
23. F. Tian, A. Prina-Mello, G. Estrada, A. Beyerle, W. Moller, H. Schulz, W. Kreyling, and T. Stoeger, *Nano Biomedicine Eng.* 1, 19 (**2009**).
24. N. Bhattarai, D. Edmondson, O. Veiseh, and F. A. Matsen, *Biomaterials* 26, 6176 (**2005**).
25. S. W. Kuo and C. J. Chen, *Macromolecules* 44, 7315 (**2011**).
26. Y. S. Lu and S. W. Kuo, *RSC Adv.* 5, 88539 (**2015**).
27. M. Sakata, D. Kato, M. Uchida, M. Todokoro, H. Mizokami, S. Furukawa, M. Kunitake, and C. Hirayama, *Chem. Lett.* 29, 1056 (**2000**).
28. D. Kato, M. Takeuchi, T. Sakurai, S. I. Furukawa, H. Mizokami, M. Sakata, C. Hirayama, and M. Kunitakea, *Biomaterials* 24, 4253 (**2003**).